

## Austenite decomposition in carbon steel under dynamic deformation conditions

**A. Nowotnik\*, J. Sieniawski, M. Wierzbńska**

University of Technology, Department of Materials Science,  
ul. W. Pola 2, 35-959 Rzeszow, Poland

\* Corresponding author: E-mail address: nowotnik@prz.edu.pl

Received 30.10.2006; accepted in revised form 15.11.2006

### Properties

#### ABSTRACT

**Purpose:** The main purpose of this paper was to estimate the effect of the dynamic conditions resulting from deformation process on the austenite decomposition into ferrite and pearlite (A→F+P) in the commercial carbon steel.

**Design/methodology/approach:** In the paper flow stress curves and microstructure of deformed steel within the range of discontinuous (austenite to pearlite) and austenite to ferrite transformation at different strain rates and cooling rates were presented. The microstructure of hot deformed samples was tested by means of an optical and electron microscopy.

**Findings:** It was shown that the flow localization during hot deformation and preferred growth of the pearlite colonies at shear bands was very limited. The most characteristic feature of the microstructure observed for hot deformed samples was the development of carbides that nucleated along elongated ferrite grains.

**Research limitations/implications:** In spite of intense strain hardening due to deformation and phase transformation overlapping, microstructural observation of deformed samples did not reveal significant flow localization effects or heterogeneous distribution of the eutectoid components. Therefore, complementary tests should be carried out on the steel with higher strain above the 0.5 value.

**Originality/value:** There was no data referred to particular features of the dynamic processes, such as dynamic recrystallization and recovery, dynamic precipitation, that can occur during austenite decomposition into ferrite, and especially during discontinuous transformation of austenite to pearlite.

**Keywords:** Mechanical properties; Carbon steel; Plastic forming; Phase transformation

### 1. Introduction

Mutual interaction between a hot deformation process and discontinuous transformation in Cu-Ti and CuNiCrSiMg alloys leads to very strong localization of deformation and dynamic coagulation of precipitates within shear bands [1-3]. It is believed that this phenomena - intensification of heterogeneous deformation - was due to discontinuous precipitation. Furthermore, it has been confirmed that microstructure of this alloys, after transformation, is morphologically similar to those in steel after decomposition of austenite to pearlite. This eutectoid transformation in steel is considered as a discontinuous one. Hence, it has been assumed that analogous effect of its localization, for the duration of hot deformation process performed within temperature of eutectoidal

transformation in particular, should take place. Analysis of structural dynamic processes proceeding in carbon steel and low alloy steel [4-14] indicates that this pertaining to the examinations carried out within the range of temperature where austenite is stable. There is a lack of data related to dynamic processes (recrystallization, recovery and precipitations) occurring directly for the period of eutectoidal decomposition. Therefore, the main aim of this work was to estimate the effect of the dynamic conditions resulting from deformation process on the eutectoidal transformation in the steel. Particular attention was focused on the microstructure and morphology of the phase components confirming non-homogenic precipitation process caused by transformation and deformation localization. The studies presented in this paper are continuation of the earlier investigations [15,16].

## 2. Material for research

Carbon steel containing (in mass fractions) 0.156%C; 0.21%Si; 0.62%Mn; 0.014%P; 0.012%S and 0.005%Al was studied. Standard cylindrical samples with dimension of  $\varnothing 5 \times 10$  mm machined from cold drawing bar of 30 mm diameter were used. The specimens were annealed at 1200°C for 30 min and then quenched into ice water. Phase transformation start and finish temperatures were determined on the base of dilatometric tests performed by means of Bähr DIL805A/D dilatometer testing equipment. The special features of the phase transformations in the examined steel are described in greater detail in [15,16].

The second set of cylindrical specimens was used for compression experiments. Hot compression tests were performed on a Bähr. Flat samples for structural observations were cut from the specimens along longitudinal axis. Thin foils were examined by means of JEOL - JEM 2010 ARP transmission electron microscope at 200kV.

## 3. Description of achieved results

In order to choose accurate conditions for following compression test, the austenite decomposition into ferrite and pearlite start ( $T_s$ ) and finish temperature ( $T_f$ ) was measured at various constant cooling rate ranged from 1°C/s to 10°C/s. These temperatures were needed to establish following deformation tests. Complete CCT diagram for examined steel can be found in following references – [15,16].

Deformation tests at predetermined cooling rate have been conducted throughout the time corresponding to the range of continuous cooling within austenite to ferrite and pearlite transformation temperature.

Hot compression tests were carried out applying roughly the identical deformation value  $\varepsilon=0.5$  at each cooling rate. For this purpose along with the increase of cooling rate the strain rate, depending on cooling time between initiation and termination of the compression test, was increased as well. The values of suitably chosen deformation conditions plotted with the part of CCT diagram showing temperature range of ferrite and pearlite, were presented in Fig. 1.

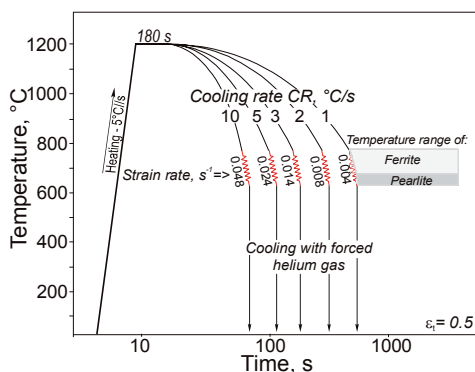


Fig. 1. Deformation scheme of compressed steel at constant strain rate of  $0.004\text{s}^{-1}$ . Strain rate was kept constant for each cooling rate by controlling the total strain of the samples – which varied from 0.15 to 0.5.

The samples were heated up to a temperature of 1200°C (austenite range) held for 180 s and cooled with a rate varied from 1, 2, 3, 5 and 10°C/s to finish temperature for a Austenite to ferrite and pearlite transformation. The steel has been hot deformed within temperatures equivalent to the range of transformations at following strain rates corresponding to the given cooling rate: 0.004, 0.008, 0.014, 0.024 i  $0.048\text{ s}^{-1}$ . Each time, total plastic strain of 0.5 was obtained. Right upon compression test termination and finishing the austenite decomposition, the samples were instantaneously cooled to room temperature with forced helium. True stress-true strain curves for deformed steel are shown in Fig. 2. One can noticed two characteristic regions:

- I – intensive strain increment at the deformation not exceeded the value of  $\varepsilon \approx 0.1$ ,
- II – uniform strain hardening increment within the range of highest deformation, that results from the effect of temperature decrease and strain hardening increase and development of phase transformation process.

Along with strain rate and cooling rate decrease, transition to the II region required lower values of deformation. The highest flow stress value was received during deformation at the highest cooling rate and strain rate -  $0.048\text{s}^{-1}$ , CR=10°C/s. Since accuracy of flow stresses measuring were to a certain extent limited, we could not unambiguously affirm if there was any essential variation of the hardening rate. Fairly gentle slope of the curves did not allow straightforwardly analyze the  $\sigma$ - $\varepsilon$  curves with the intention of determination of characteristic ranges of temperature for given stages of decomposition of austenite into ferrite and pearlite.

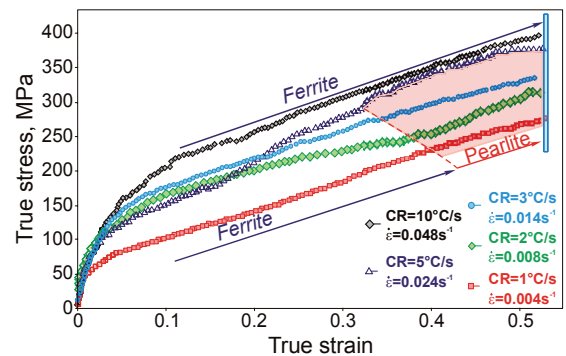


Fig. 2. True stress – true strain curves received during continuous cooling within the temperature range of austenite to ferrite and pearlite transformation

Microstructure of the sample deformed at true strain rate of  $0.008\text{s}^{-1}$  revealed a mixture of strongly deformed ferrite and pearlite with insignificant amounts of bainite. Predominant constituents of the microstructure is ferrite (Fig. 3a). It was concluded that rather slow cooling rate and low strain rate did not promote any preferential distribution of phase components.

One should notice that microstructure of the steel created by a given deformation conditions, that is rather slow cooling rate and low strain rate was mostly uniform. No regions, where eutectoidal transformation could be localized due to nucleation of the phases in the sites assigned to localization of deformation, has been observed.

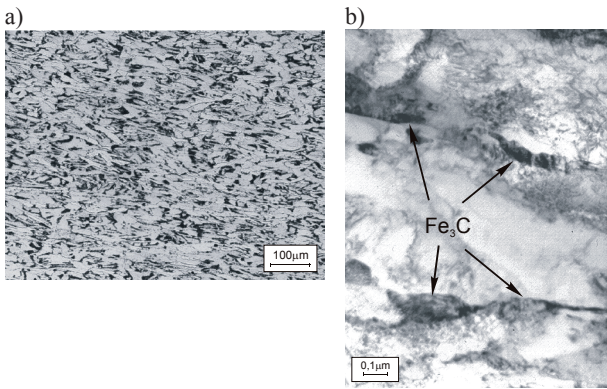


Fig. 3. Microstructure of the sample deformed  $\epsilon=0.5$  during austenite decomposition into ferrite and pearlite at cooling rate of  $2^\circ\text{C/s}$  and strain rate of  $0.0008\text{s}^{-1}$ : a) light microscope, b) TEM micrograph

TEM observations of this sample indicate the presence of numerous cementite precipitates distributed along the ferrite grain boundaries which are probably formed (spread) at the migrated grain boundary - austenite to ferrite transformation front (Fig. 3b). This may suggest both substantial intensiveness of carbides nucleation along boundary front and strong retardation of ferrite grains growth (cementite particles act as obstacles to grain boundaries migration). Most of them have a slightly elongated shape. Similar effect of the cementite distribution at elongated ferrite grains was observed in the steel deformed at higher strain rate  $0.014\text{s}^{-1}$  and cooling rate of  $3^\circ\text{C/s}$ . It appears that in the most cases carbides in the deformed steel form colonies arranged at various angle to the deformation direction (axis of the sample).

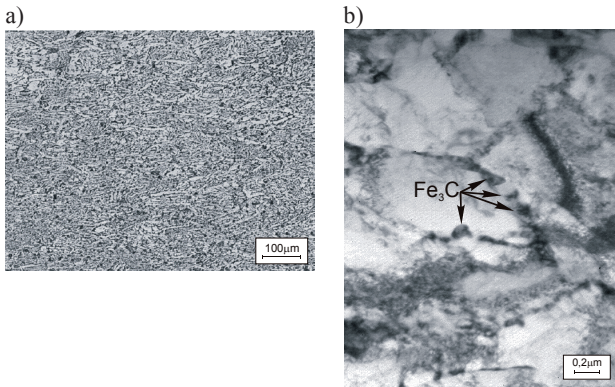


Fig. 4. Steel deformed during austenite to ferrite and pearlite transformation at cooling rate of  $10^\circ\text{C/s}$  and strain rate of  $0.048\text{s}^{-1}$

It was found that the increase of strain rate and accelerated cooling during deformation is conducive to formation of a bainite. At strain rate of  $0.048\text{s}^{-1}$  and cooling rate of  $10^\circ\text{C/s}$ , the microstructure of the steel consists a ferritic-bainitic structure with the predominant amount of the bainite (Fig. 4a). Light microscopy observations did not reveal any obviously effects of the microstructure components arrangements that might have resulted from privileged nucleation of carbides in the sites of non-homogenic deformation. In addition to this sample, TEM observation also (similarly to the sample deformed at

lower strain rate) reveals intensive effect of carbides formation along ferrite grain boundaries (Fig. 4b).

It was concluded that relatively slow cooling rate and low strain rates did not practically cause any localization of  $A \rightarrow F+P$  phase transformation. For this reason few more attempt was made to intensify microstructural processes changing deformation conditions during austenite to ferrite and pearlite decomposition.

Therefore, complementary hot compression experiments were carried out on the samples cooled with constant cooling rate ranging from 1 to  $5^\circ\text{C/s}$  and deformed within start and finish transformation temperature range. As a constant strain rate was used, samples were deformed with varied true strain from 0.15 to 0.5 depending on the “passage time” through the phase transformation region (Fig. 5).

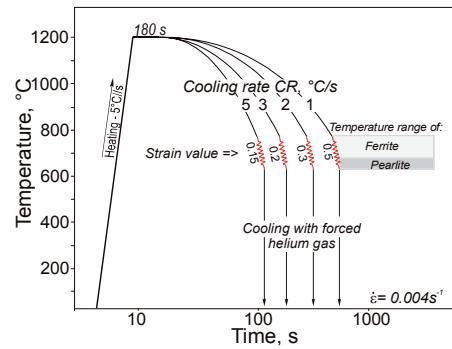


Fig. 5. Scheme of laboratory processing schedules. Samples were deformed at a strain rate of  $0.004\text{s}^{-1}$ . Final deformation of the sample was dependent on the time passing through the austenite decomposition temperature range marked on the figure

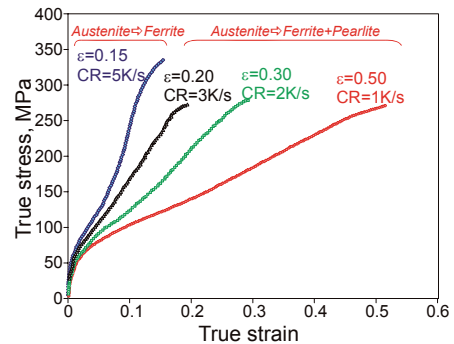


Fig. 6.  $\sigma$ - $\epsilon$  curves received during deformation at various strain values within A-F+P transformation

True stress/true strain curves for samples deformed at different cooling rates are shown in Fig. 6. Hardening rate as well the final flow stress value was found to increase with increasing cooling rate in spite of reduced deformation of the sample. As the strain rate was the same for each experiment, one can conclude that the hardening rate depends mostly on refining of the structure components due to phase transformation being accelerated with increasing cooling rate. In particular, an effective hardening effect at largest cooling rate of  $5^\circ\text{C/s}$  can be ascribed to the ferrite grain refinement as well as early stage of bainite development at the end of compression test. Light and transmission electron microscopy (TEM) observations performed for

the sample deformed with relatively low cooling rate ( $1^{\circ}\text{C/s}$ ) and low strain rate did not practically reveal any shear bands development that would provide preferential sites for nucleation of pearlite or ferrite grains. Microstructural components have shown a random distribution in the material structure (Fig. 7a).

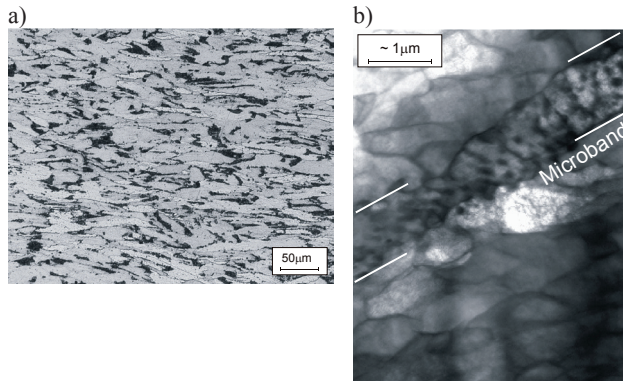


Fig. 7. (a) microstructure of the sample deformed  $\varepsilon=0.5$  at cooling rate of  $1^{\circ}\text{C/s}$  and strain rate of  $0.004\text{s}^{-1}$ ; (b) bainite and pearlite distributed along shear band in the sample deformed  $\varepsilon=0.3$  at cooling rate of  $3^{\circ}\text{C/s}$  and strain rate of  $0.004\text{s}^{-1}$

TEM observations of the same sample confirmed practically uniform distribution of structural components at the sample deformed at higher cooling rate. Any noticeable shear bands development and related preferential nucleation of pearlite or ferrite grains were found. TEM observations evidenced very few effects of non-uniform distribution of microstructural components that might result from preliminary flow localization (Fig. 7b). Elongated pearlite and bainite colonies development can be related to the flow localization and accelerated phase transformation along shearing area. This is however rarely observed effect of structural heterogeneity that might be related to localized plastic flow and discontinuous transformation of  $\text{A} \rightarrow \text{F} + \text{P}$ . It is worth to stress that the most distinguishable feature of the all samples structure is related to privileged  $\text{Fe}_3\text{C}$  particles distribution along elongated ferrite boundaries.

## 4. Conclusions

1. It was shown that the flow localization during hot deformation and preferred growth of the pearlite colonies at shear bands was very limited.
2. Localized  $\text{Fe}_3\text{C}$  particles development at ferrite grain boundaries was often observed for almost all samples deformed within the range of transformation. TEM observations lead to a conclusion that the effect described above is the most essential feature of the localized form of nucleation during phase transformation and simultaneous deformation of the sample.

## Acknowledgements

This work was carried out with the financial support of the Ministry of Science and Higher Education under grant No. N507 115 31/2788.

## References

- [1] M. Niewczas, E. Evangelista, L. Błaż, Strain localization during a hot compression test of Cu-Ni-Cr-Si-Mg alloy, *Scripta Metallurgica et Materialia*, 27 (1992) 1735-1740.
- [2] A.A. Hamed, L. Błaż, Microstructure of hot-deformed Cu-3.45 wt.% Ti alloy, *Materials Science and Engineering*, A254 (1998) 83-89.
- [3] A.A. Hamed, L. Błaż: *Scripta Materialia*, Flow Softening During Hot Compression of Cu-3.45wt.%Ti Alloy, 12 (1997) 1987-1993.
- [4] J.J. Jonas, I. Weiss, *Material Science and Engineering*, Effect of precipitation on recrystallization in microalloyed steels, 13 (1979) 238-245.
- [5] A. Korbel, W. Bochniak, F. Ciura, H. Dybiec, K. Piela, Proceedings: Sessions and Symposia sponsored by the Extraction and Processing Division, held at the TMS Annual Meeting in Ontario, Florida USA, (1997) 301-312.
- [6] A. Korbel, W. Bochniak, F. Ciura, H. Dybiec, K. Piela, The 'natural' metal-matrix composite formation by thermo-mechanical treatments, *Journal of Materials Processing Technology*, 78 (1998) 104-111.
- [7] A.K. Lis, J. Lis, High strength hot rolled and aged microalloyed 5%Ni steel, *Journal of Achievements in Materials and Manufacturing Engineering*, 18 (2006) 37-42.
- [8] L. Skálová, R. Divišová, D. Jandová, Thermomechanical processing of low alloy TRIP steel, Proceedings of the 12<sup>th</sup> Scientific International Conference AMME'2003, Gliwice-Zakopane, 2003, 249-252.
- [9] D. Jandová, Influence of hot and warm deformation on austenite decomposition, *Journal of Achievements in Materials and Manufacturing Engineering*, 18 (2006) 375-378.
- [10] D. Jandová, J. Rehor, Z. Nový, Microstructural changes taking place during the thermo-mechanical processing and cold working of steel 18Cr18Mn0.5N, *Journal of Materials Processing Technology*, 157-158 (2004) 523-530.
- [11] M. Jabłońska, K. Rodak, G. Niewielski, Characterization of the structure of FeAl alloy after hot deformation, *Journal of Achievements in Materials and Manufacturing Engineering*, 18 (2006) 107-110.
- [12] Hou, Huoran, Chen, Qi'an, Liu, Qingyou, Dong, Han, Grain refinement of a Nb-Ti microalloyed steel through heavy deformation controlled cooling, *Journal of Materials Processing Technology*, 137 (2003) 173-176.
- [13] J. Adamczyk, M. Carsi, R. Kozik, R. Wusatowski, Structure evolution during hot deformation of a C-Mn-V-N steel grade, *Journal of Materials Processing Technology*, 53 (1995) 15-22.
- [14] L. Berkowski, The influence of warm plastic deformation on the structure and on the applicable properties of high speed steel, *Journal of Materials Processing Technology*, 60 (1996) 637-641.
- [15] A. Nowotnik, L. Błaż, J. Sieniawski, Phase deformation in 0.16% C steel under hot deformation conditions, Proceedings of the Seminar Devoted to the 70th Birthday Anniversary of Prof. Z. Jasiński, Kraków 2005, 213-218.
- [16] A. Nowotnik, L. Błaż, J. Sieniawski, Interaction of phase transformation and deformation process during hot deformation of 0.16% C steel, *Defect and Diffusion Forum*, 237-240 (2005) 1240-1245.